Spectrally combined blue diode lasers pumping a Pr^{3+}:YLF crystal

YU LIU[1], XINGYU CUI[1], HONG LEI[1,2,3], QIANG LI[1,2,3], ZHANDA ZHU[1,2,3,*]
[1]*Institute of Laser Engineering, School of Physics and Optoelectronic Engineering, Beijing University of Technology, Beijing 100124, China*
[2]*Key Laboratory of Trans-scale Laser Manufacturing Technology, Ministry of Education, Beijing 100124, China*
[3]*Beijing Engineering Research Center of Laser Technology, Beijing 100124, China*

To achieve higher-power visible laser output from a Pr^{3+}:YLF crystal, we introduced, for the first time, spectral beam combination of blue laser diodes to overcome individual diode power limitations. By optimizing key parameters including the output mirror's transmittance and curvature, a maximum output power of 7.95 W at 639.5 nm was obtained under 20 W of pump power, corresponding to an optical-to-optical efficiency of 42.31%. This demonstrates the feasibility of scaling visible laser power using Pr^{3+}:YLF crystals pumped by spectrally combined blue diodes.

(Received January 30, 2026; accepted June 2, 2026)

Keywords: Blue laser diodes, Spectral beam combining, Pr^{3+}:YLF, Visible lasers

1. Introduction

In recent years, with the rapid development of visible lasers (operating in the 390–780 nm wavelength range), these lasers have been extensively applied in diverse fields including medical treatment [1], holographic display technology [2], and optical communication [3]. The exceptional monochromaticity, directionality, and brightness of visible lasers enable RGB display systems to produce sharp, high-contrast images. Furthermore, high-power all-solid-state red lasers serve as ideal pump sources for femtosecond Kerr-lens mode-locked lasers based on Cr:LiSAF crystal [4].

Among rare-earth ions, Pr^{3+} exhibits multiple energy level transitions that cover a large part of the visible spectrum. Its absorption peaks are primarily located around 444 nm and 480 nm. Recently, the advancement of InGaN blue diode lasers (emitting around 440–450 nm) provided an excellent spectral match to the absorption peaks of Pr^{3+}, significantly boosting the development of Pr^{3+}-doped lasers.

In 2004, Richter et al. demonstrated for the first time the pumping of a Pr^{3+}:YL crystal using an InGaN blue laser diode, achieving red laser emission at 639.7 nm [5]. In 2011, the research group of G. Huber at the University of Hamburg obtained 0.938 W of output at 639.5 nm [6]. In 2016, S. Luo et al. from Xiamen University utilized blue laser diodes to pump two Pr^{3+}:YLF crystals with different specifications (4.8 mm-0.5 at.% and 8 mm-0.2 at.%). The M^2 factors of the pump beam were measured to be 25.7 and 12.3 along two orthogonal directions. This system achieved a laser output of 640 nm with a power of 2.3W [7], accompanied by excellent beam quality factor $M^2 < 1.5$. In 2018, Tanaka et al. from Keio University employed four 5 W blue LDs ($M^2 \approx 20 \times 2$) to pump the gain medium, achieving 6.7 W at 640 nm [8]. In 2021, Lin Xiuji et al. from Xiamen University utilized a laser diode with $M^2_x = 46.91$ and $M^2_y = 15.53$ as the pump source, achieved 8.14 W output at 639 nm. The beam quality factors of the output laser were $M^2_x = 3.3$ and $M^2_y = 1.1$ [9].

Currently, a single blue LD typically delivers an output power of approximately 5 W, and such low pump power has become one of the key factors restricting the development of Pr^{3+}:YLF red lasers. While spatial beam combining of diode arrays can increase the power, it often results in the degradation of the beam quality, which in turn reduces the efficiency. This is primarily due to the considerable influence of the waist radius of pump beam on the mode-matching efficiency. Effective mode matching requires that the fundamental mode radius w_1 of the oscillating laser should be no smaller than the pump spot radius w_p [10]. Thus, improving the pump beam quality is essential for enhancing mode-matching performance.

Conventional techniques such as polarization beam combination and dual-end pumping are commonly used to boost the total pump power; however, these methods can only increase the power by up to four times, failing to meet the demand for higher power scaling. Currently, the spectral beam combining technology for semiconductor lasers mainly focuses on the 800 nm and 900–1000 nm waveband [11-13]. Research reports on the spectral beam combining technology for blue semiconductor lasers are relatively scarce.

In this experiment, the spectral beam combination technique for blue laser diodes (LDs) was first adopted to enhance pump power without compromising the pump beam quality. Each individual LD emitter delivers a maximum output power of approximately 3 W, and spectral combination of nine such emitters achieves a total output power of around 25 W. Furthermore, if conventional polarization beam combination and dual-end pumping are further integrated, the total pump power can exceed 100 W—while the beam quality of the combined pump beam remains nearly comparable to that of a single emitter. This approach provides an effective pathway for achieving a substantial boost in visible laser power.

2. Experimental

2.1. The basic characteristics of Pr^{3+}:YLF crystal

Fig. 1 illustrates the energy-level structure and visible-wavelength transitions characteristic of Pr^{3+}. The absorption and emission spectral properties of Pr^{3+}:YLF are presented in Table 1. The emission cross-section of Pr^{3+}:YLF at 640 nm is 2.2×10^{-19} cm², which is larger than those at other wavelengths [14]. This high emission cross-section not only benefits laser oscillation but also provides favorable conditions for high-power laser operation. The emission cross-sections were calculated using the Füchtbauer-Ladenburg formula.

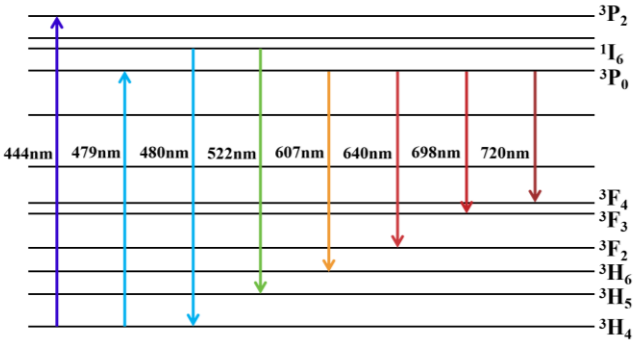

Fig. 1. Energy level structure of Pr3+ and level transitions in visible laser band (colour online)

Fig. 2 shows the π-polarized absorption spectrum of the Pr^{3+}:YLF crystal and the spectrum of the pump laser. As shown in Fig. 2 the crystal exhibits three strong absorption peaks at 443.9 nm, 468 nm, and 479.4 nm, with the strongest one centered at 443.9 nm—corresponding to the $^3H_4 \rightarrow {}^3P_2$ transition of Pr^{3+}. Therefore, the pump source used in this experiment has a central wavelength in the range of 442-447, achieving an excellent spectral match with the absorption peaks of the Pr^{3+}:YLF crystal.

Table 1. Cross-sections of Pr^{3+}:YLF

	λ in nm	σ in 10^{-19} cm^2
Absorption	443.9	0.9
	468	0.6
	479.4	2.0
Emission	479	1.9
	523	0.3
	607	1.4
	640	2.2
	698	0.5
	721	0.9

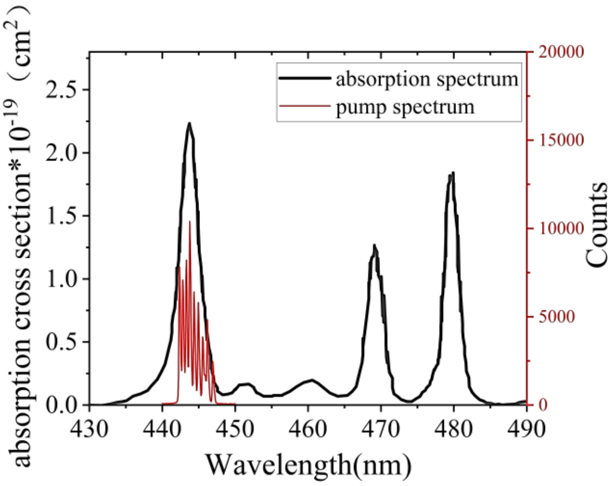

Fig. 2. π-polarized absorption spectrum of Pr3+:YLF and pump laser spectrum (colour online)

2.2. Experimental setup

Fig. 4 depicts the experimental setup for the Pr^{3+}:YLF red laser. The pump source is a tunable external cavity semiconductor laser consisting of nine LDs of the same model, with beam quality factors of $M^2_x = 1.2$ and $M^2_y = 8$. The laser operates within a wavelength range of 440±10 nm and possesses a broad gain bandwidth, which ensures a sufficiently wide wavelength locking range. The front facet reflectivity of the semiconductor laser chip is approximately 1%, which facilitates the efficient injection of feedback light into the cavity and enables easy wavelength locking.

The emission wavelength of the blue LD at different injection currents was measured using a spectrometer, as shown in Fig. 3. It can be observed that as the injection current increases from 1.2 A to 2.8 A, the central wavelength of the pump source shifts from 446.3 nm to 449.4 nm in free running mode. After wavelength locking, the central wavelength stabilizes around 444 nm.

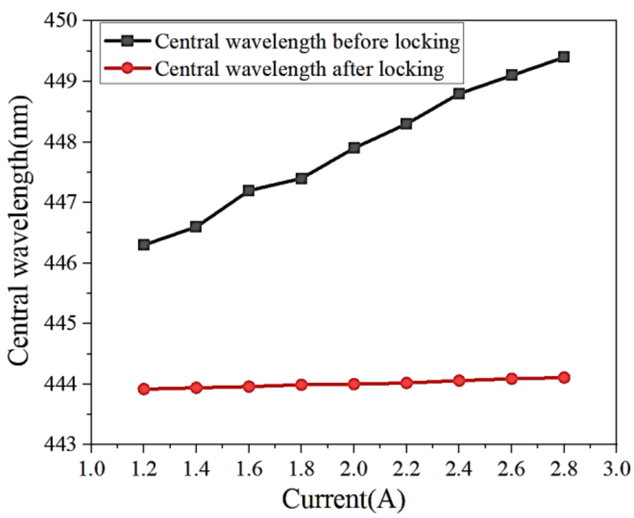

Fig. 3. Central wavelength before and after wavelength locking (colour online)

The pumping beams emitted from the blue laser diode were collimated along both the fast and slow axes. A plano-convex cylindrical lens with a focal length of 400 mm was used as a transform lens to redirect the beams toward a diffraction grating. The beams were incident at different angles and focused on the same position. The grating utilized its angular dispersion to direct all beams into a common exit angle. The combined beam exhibited a beam quality identical to that of a single LD emitter, while the total output power was the sum of the individual emitters. The collimating lens forms the beam into a parallel profile, ensuring parallel propagation upon its incidence on the output mirror. An output coupler was used to reflect a part of the light back into the cavity for feedback, while allowing the remainder to be transmitted as output. Oscillation and wavelength locking were achieved between the output coupler and the rear facet of the laser emitters, thereby completing the spectral beam combination process. The combined pump beam reached a maximum output power of 25 W, with beam quality factors of M^2_x = 1.4 and M^2_y = 13.

The spot sizes of the blue LDs were significantly asymmetrical between the horizontal and vertical directions. To mitigate the astigmatism effects, the pump beam was optimized. The calculated beam radii at the waist were 3.9 mm along the fast axis and 0.87 mm along the slow axis. A cylindrical lens pair with focal lengths of 50 mm and –12.7 mm was used to compress the fast-axis spot size to one-fourth of its original radius, making it comparable to the spot size in the slow-axis. This optimization results in a symmetrized spatial profile of the pump beam, reduced astigmatism, and improved mode matching. Subsequently, the beam was focused into the crystal via a spherical focus lens (F = 50 mm).

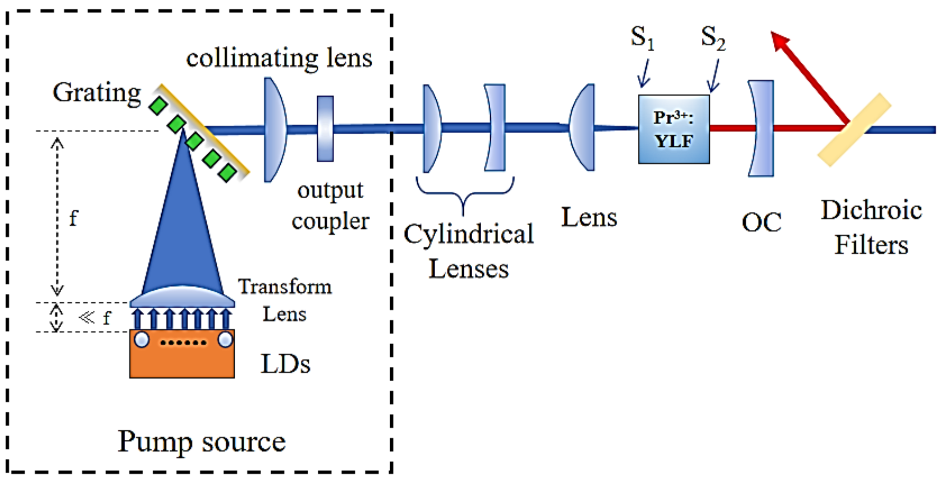

Fig. 4. Schematic of the experimental setup (colour online)

To minimize losses from additional cavity mirrors and simplify the resonator structure, the S_1 face of the Pr^{3+}:YLF crystal was coated to function as an input mirror, with high reflection (HR) at 640 nm and anti-reflection (AR) at the blue pump wavelength. The opposite S_2 face was coated with dual-band AR coatings for both 640 nm and the blue wavelength. The crystal was cut along the a-axis (0.5 at.%, 3 mm × 3 mm × 22 mm). It was mounted on a copper block heat sink, which was maintained at 20°C via water cooling. The 639 nm output laser was extracted through the output coupler (OC). A dichroic mirror serving as a short-pass filter was utilized to reflect the 639 nm laser toward a power meter for output power measurement.

3. Results and discussion

Fig. 5 shows the spectrum of the pump source used in this experiment. Its peak wavelength falls within the 442–447 nm band, which is centered near the absorption peak of the Pr^{3+}:YLF crystal.

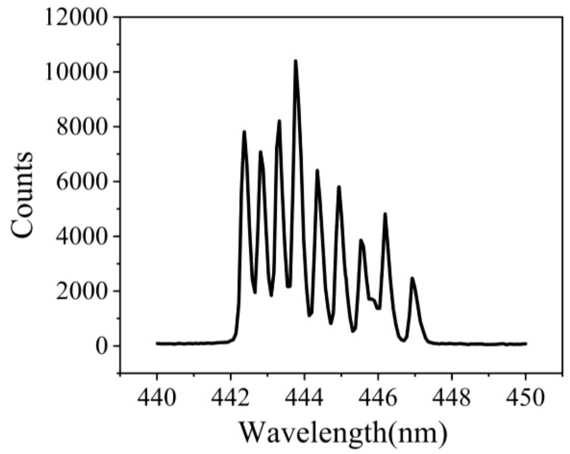

Fig. 5. Pump laser spectrum

The absorbed pump power of the 22 mm crystal was measured, and the specific absorption characteristics are shown in Fig. 6. At an input power of 20 W, the absorption efficiency is 81%, which meets the target of 80% absorption efficiency.

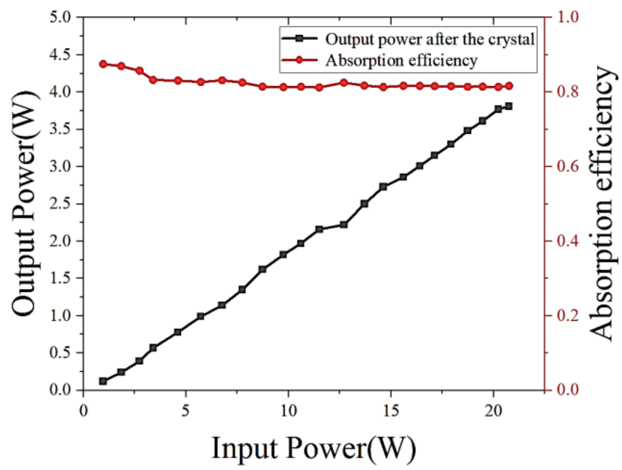

Fig. 6. Absorption power of the 22 mm crystal (colour online)

To maximize the output power at 640 nm, the output coupler (OC) was optimized by adjusting its parameters to improve mode matching between the pump and laser beams, thereby achieving the highest possible output. The OC used was a plano-concave mirror with curvature (30 mm, 50 mm, and 100 mm), and three different transmittance coatings (2%, 5.2%, and 8%) at 640 nm were applied to examine the output characteristics of the red laser under different conditions. The corresponding output performance is shown in Fig. 7.

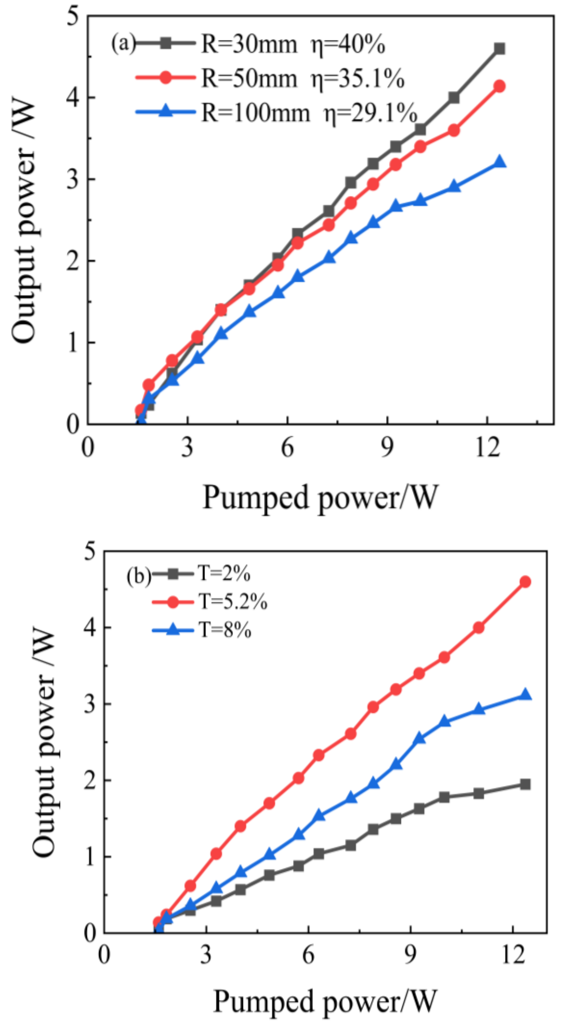

Fig. 7. Comparison of red laser output performance under different parameter conditions. (a) The red laser output performance of the OC under 5.2% transmittance and different curvatures (30 mm, 50 mm and 100 mm); (b) Red laser output performance of the OC under 50 mm curvature and different transmittances (2%, 5.2% and 8%) (colour online)

As shown in Fig. 7 (a), when comparing the output performance of output couplers (OC) with different radii of curvature while keeping the same transmittance constant at 5.2%, the highest red output power of 4.6 W was achieved with a curvature radius of R_{OC} = 30 mm, corresponding to a slope efficiency of 40%. Using an output coupler with R_{OC} = 50 mm, the output power dropped to 4.14 W, with a corresponding slope efficiency of 35.1%. For the OC with R_{OC} = 100 mm, the output power and slope efficiency further decreased to 3.2 W and 29.1%, respectively.

A comparison of output power was also conducted for OC with the same curvature (50 mm) but different transmittance, as shown in Fig. 7 (b). The results indicate that the optimal output performance was achieved with an output coupler transmittance rate of T_{OC} = 5.2%. Based on this, an output coupler with a curvature of R_{OC} = 30 mm and transmittance rate of T_{OC} = 5.2% was selected as the optimal configuration for higher-power pumping experiments.

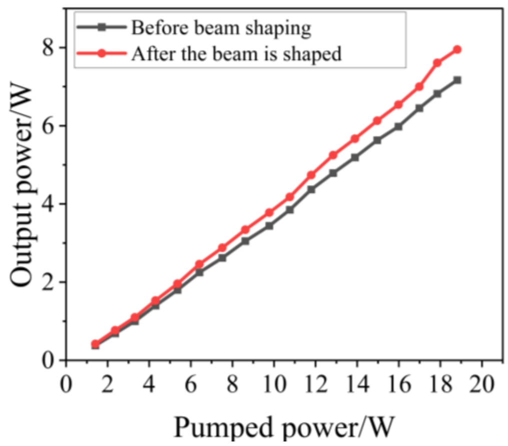

Fig. 8. The performance of red laser output under optimal parameter conditions (colour online)

The output characteristic curves after compressing the fast-axis pump laser spot are presented in Fig. 8. The two curves correspond to the output power with and without beam shaping, respectively. At a pump power of approximately 19 W, the maximum output powers reached 7.95 W and 7.17 W, with corresponding optical-to-optical efficiencies of 42.31% and 38.12%. This result clearly demonstrates the effectiveness of fast-axis pump spot compression in enhancing laser performance.

Spectral analysis of the red laser output was conducted using a spectrometer; as shown in Fig. 9, the measurement results reveal a central wavelength of 639.5 nm and a full width at half maximum (FWHM) of approximately 0.3 nm.

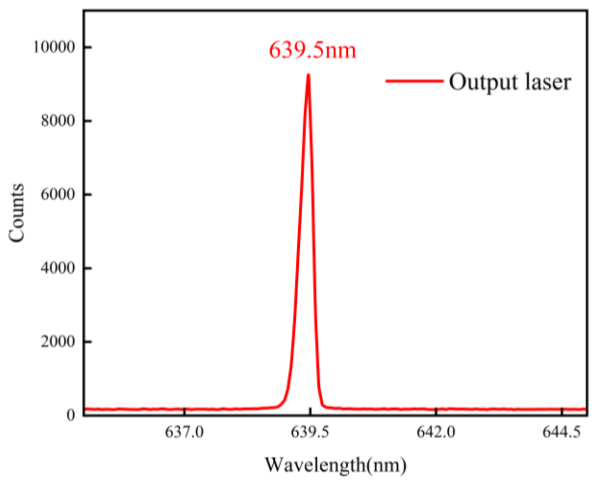

Fig. 9. Spectrum of output laser (colour online)

4. Conclusion

This study presents a 640 nm red laser system pumped by a spectrally combined blue laser diode. A maximum output power of 7.95 W was achieved, with an optical-to-optical efficiency of 42.31%. By adopting spectral beam combining, the pump power was enhanced while retaining excellent beam quality—laying the groundwork for higher output power. This approach effectively mitigates the poor beam quality issue commonly encountered when using diode laser arrays for pumping, providing a solid foundation for further power scaling. Future work may involve integrating polarization beam combination or dual-end pumping to further boost pump power, as well as increasing the number of combined emitters in the spectral beam combining system. Notably, the Pr^{3+}:YLF crystal fractured when the pump power reached 20 W in our experiments, which is attributed to significant thermal effects induced by high-power pumping. Future research should also focus on mitigating thermal effects and developing new materials of crystal to achieve higher power pumping.

Acknowledgements

This work is supported by the Natural Science Foundation of Beijing, China (Grant No. L241060).

References

[1] S. P. Nistico, M. Tolone, T. Zingoni, F. Tamburi, E. Scali, L. Bennardo, G. Cannarozzo, Photobiomodulation, Photomedicine, and Laser Surgery **38**(9), 560 (2020).
[2] K. Yamamoto, Advanced Optical Technologies **1**(6), 483 (2012).
[3] G. Y. Hu, C. Y. Chen, Z. Q. Chen, Journal of Zhejiang University-Science A **8**(2), 186 (2007).
[4] S. A. Payne, L. K. Smith, R. J. Beach, B. H. T. Chai, J. H. Tassano, L. D. DeLoach, W. L. Kway, R. W. Solarz, W. F. Krupke, Applied Optics **33**(24), 5526 (1994).
[5] A. Richter, E. Heumann, E. Osiac, G. Huber, W. Seelert, A. Diening, Optics Letters **29**(22), 2638 (2004).
[6] T. Gün, P. Metz, G. Huber, Optics Letters **36**(6), 1002 (2011).
[7] S. Y. Luo, X. G. Yan, Q. Cui, B. Xu, H. Xu, Z. Cai, Optics Communications **380**, 357 (2016).
[8] H. Tanaka, S. Fujita, F. Kannari, Applied Optics **57**(21), 5923 (2018).
[9] X. J. Lin, M. P. Chen, Q. C. Feng, S. Ji, S. Cui, Y. Zhu, B. Xiao, W. Li, H. Xu, Z. Cai, Optics & Laser Technology, **142**, 107273 (2021).
[10] T. Y. Fan, A. Sanchez, IEEE Journal of Quantum Electronics **26**(2), 311 (1990).
[11] J. Zhang, H. Peng, X. Fu, Y. Liu, L. Qin, G. Miao, L. Wang, Optics Express **21**(3), 3627 (2013).
[12] Q. Zhou, C. Zhou, N. Yu, C. Wei, W. Jia, Y. Lu, Chinese Optics Letters **15**(9), 091403 (2017).
[13] Z. Zhu, L. Gou, M. Jiang, Y. Hui, H. Lei, Q. Li, Optics Express **22**(15), 17804 (2014).
[14] A. Richter, E. Heumann, G. Huber, V. Ostroumov, W. Seelert, Optics Express **15**(8), 5172 (2007).

*Corresponding author: zhuzhanda@126.com